

Frequency analysis of random fatigue: Setup for an experimental study

Michele Sgamma | Andrea Chiocca | Francesco Bucchi | Francesco Frendo

Department of Civil and Industrial Engineering, University of Pisa, Pisa, L. Lucio Lazzarino, Italy

Correspondence

Michele Sgamma, Department of Civil and Industrial Engineering, University of Pisa, Pisa, L. Lucio Lazzarino 56122, Italy.
Email: michele.sgamma@phd.unipi.it

Abstract

The frequency-domain approach to fatigue life estimation in random loading has been largely investigated due to its computational advantages, and several methods for the frequency translation of the most common time-domain methods have been proposed. Between the most known frequency methods, there are Bendat's method, valid for narrow-band signals, and Dirlik's formula, which is considered the best result for wide-band signals. However, a great part of the frequency methods takes the rainflow count as a reference time-domain method and uses the rainflow damage computation as the exact value to emulate. Therefore, very few experimental data for the fatigue life of mechanical components subject to random loads are available in the literature. This work presents the setup for a series of experimental tests for specimens subjected to random loads, aiming at achieving experimental data to compare with the results provided by frequency methods. After a brief description of the materials used for the setup, the two-step test concept is described: first, the specimen will be subjected to random loads obtained by a certain power spectral density for an amount of time which should nominally cause a 30% of damage; then, the fatigue test will be ended on a resonance testing machine to compute the actual residual fatigue life of the specimen; this two-step testing also allows to reduce the time requested for the tests. The test bench developed for the experimental investigation is described in the paper, together with the results of some preliminary tests, aimed at verifying the feasibility of the conceived procedure.

KEYWORDS

durability, experimental tests, frequency analysis, random fatigue, structural analysis

INTRODUCTION

The evaluation of the fatigue damage of structures or components subjected to random loads is a matter of very high importance for many manufacturers. Indeed, during the design phase, very often the designers have to match with stochastic loads, for example, road surface, aerodynamic or fluid dynamic loads, such as those induced by wind or sea waves. These stochastic loads cannot be dealt with as they are deterministic, because it would require the use of very high

safety coefficients, leading to an increase in both cost and weight for the product. To avoid this, there is the need to determine some profiles that are statistically representative of the random load. Anyway, these profiles are very long, and they are not made by a lot of repetitions of the same loading condition, but they present a wide variety that has to be determined separately. This type of analysis would require very long computational time in time domain, especially if we have to repeat the calculations for different points of the mechanical component. To reduce the demand for

computational effort, a possible solution is to move the fatigue analysis to the frequency domain. The frequency domain, in fact, is inherently characterized by higher computational efficiency and also allows exploitation of the properties of the power spectral density (PSD), which is the most comprehensive and efficient method of representing a random load.

As just mentioned, the starting point for frequency analysis of fatigue is the PSD of the stress on the component. The PSD can be related to the features of the load in the time domain by calculating the spectral moments [1], which are defined as integrals of various orders of the PSD. One of the main parameters that depend on the spectral moments is the irregularity factor, that is, a measure of the bandwidth of the random signal. The frequency methods for fatigue analysis use the spectral moments to estimate the probability density function (pdf) of the amplitudes of the cycles of the stress signal, which is the same output that we would obtain from a time-domain cycle counting method, and from which it is possible to compute the damage using, for example, the Palmgren-Miner rule for damage accumulation. Despite the difficulty of this step in the frequency domain, there are several methods that, under certain hypotheses, led to fairly accurate results. The main theoretical result has been provided by Bendat [2], who proposed a Rayleigh function to approximate the amplitude pdf of cycles for narrow-band signals. To extend the results of Bendat's theory to wide-band signals, several authors [3–6] proposed corrective coefficients for the damage value, based on spectral moments of various orders and on the slope of the fatigue curve of the material. Despite that, the most important results for wide-band random loads came from Dirlik's formula [7], which managed to approximate with low error the marginal amplitude pdf of counted cycles for a very wide range of signal bandwidth.

However, a great part of the frequency methods takes the rainflow count [8] as a reference time-domain cycle counting method and uses the rainflow damage computation as the exact value to emulate. Therefore, very few experimental data for the fatigue life of mechanical components subject to random loads are available in the literature [9–13], and most of them are obtained for particular conditions of loading (multiaxial or non-Gaussian stress state) or for special shapes of the specimen (Y-shaped, notched, etc.). Niestony et al. [9], in 2012, published the results of 107 experimental tests made on tubular specimens with a one-sided hole subjected to complex multiaxial random loads. In 2021, Marques et al. [10] performed a series of experimental tests on aluminum sheets subjected to random bending loads to validate the effectiveness of their methodology for structural health monitoring of fatigue cracks under stationary random loads. Gao et al. [11] proposed in the same year a new method for spectral analysis of fatigue due to multiaxial random loads with mean stresses, and they verified their method by making some experimental tests on notched plate specimens made of aviation-grade aluminum alloy. A similar geometry for the specimens was used by Wang and Serra [12], who performed a small number of acceleration-driven random tests on one-side constrained double-notched beam specimens to validate a previously presented numerical method for non-Gaussian random loading. Finally, Palmieri et al. [13] made some

experimental fatigue tests on three-dimensional (3D)-printed Y-shaped specimens, with their base mounted on an electrodynamic shaker and two masses fixed on their arms, to check the validity of spectral methods for 3D-printed polylactic acid samples.

In addition to the reliance on the rainflow count, a further reason for the lack of experimental data lies in the difficulty of performing experimental random fatigue tests on standard specimens. In fact, the resonance testing machines commonly used for fatigue testing allow only constant amplitude and frequency tests; while, on the other hand, shakers, that is, the dynamic machines commonly used to apply random loads, are generally used only for acceleration-driven dynamic tests on single-ended constrained systems.

This work aims to propose and test an experimental setup for normal stress fatigue tests on standard specimens subjected to random loads to achieve experimental data that can be compared with both the results provided by frequency methods and the results obtained by typical constant amplitude fatigue tests.

FREQUENCY ANALYSIS OF RANDOM LOADS

The starting point of fatigue analysis in the frequency domain is the PSD of the load. The PSD is a scalar function that describes how the power of a given signal is distributed among the frequencies and it is the most complete and efficient way to represent a stationary random load. This representation of the signal in the frequency domain is related in various ways to its time-domain representation, and the tools to express these relationships are the spectral moments, calculated by integrating the PSD. The spectral moment of n th order is given by

$$\lambda_n = \int_0^{\infty} \omega^n G(\omega) d\omega,$$

where $G(\omega)$ is the PSD of the signal and ω is the angular frequency in rad/s.

The standard deviation σ_x of a random signal is equal to the square root of the zero-order spectral moment, that is to say that the variance of a time signal can be calculated by the integral of its PSD. According to Rice's formulas [14], it is possible to relate the PSD to two more important time-domain properties of the stochastic signal using the spectral moments of order 0, 2, and 4: the mean up-crossing rate v_0 and the rate of peak occurrence v_p

$$v_0 = \frac{1}{2\pi} \sqrt{\frac{\lambda_2}{\lambda_0}}, \quad v_p = \frac{1}{2\pi} \sqrt{\frac{\lambda_4}{\lambda_2}}.$$

The ratio between these two parameters defines one of the principal parameters for frequency fatigue analysis: the irregularity factor γ , which is a measure of how much the process is concentrated around a central frequency:

$$\gamma = \frac{v_0}{v_p} = \frac{\lambda_2}{\sqrt{\lambda_0 \lambda_4}}.$$

An irregularity factor near unity is typical of narrow-band signals, which are characterized by a single predominant frequency, and have a number of peaks per second very close to the number of mean up-crossings per second. Despite this case is not so frequent in real random loading conditions, it is still interesting to be studied owing to Bendat's theory [2], which is valid only for narrow-band signals and provides the most important theoretical result for the frequency translation of time-domain counting methods. In fact, from this hypothesis, Bendat derived that the amplitude of each cycle can be considered equal to the peak of the cycle signal and managed to estimate the pdf of the amplitudes S of the cycles with a Rayleigh distribution only dependent on the zero-order moment of the signal PSD

$$p(S) = \frac{S}{\lambda_0} e^{-\frac{S^2}{2\lambda_0}}.$$

On the other side, wide-band signals have a number of peaks that is higher than the number of mean up-crossings, thus bringing decreasing values of the irregularity factor as the frequency span of the signal PSD increases. In case of wide-band signals, the results provided by Bendat's theory are no more acceptable, since it overestimates the total fatigue damage [15, 16]. To overcome this problem, several authors provided corrective coefficients to be multiplied directly to the damage value calculated using Bendat's formula, to extend its use to wide-band random loads [3–6]. However, the most accurate results have been obtained by other authors who tried to give new definitions for the marginal amplitude pdf, based on several higher-order spectral moments [7, 17, 18]. The most accurate results were obtained by Dirlik [7], who used a Monte Carlo approach to define the amplitude pdf of the cycles as a combination of an exponential distribution and two Rayleigh distributions, all depending on the first 4 spectral moments of the signal PSD:

$$p(z) = \frac{\frac{D_1}{Q} e^{-\frac{z}{Q}} + \frac{D_2}{R^2} z e^{-\left(\frac{z^2}{2R^2}\right)} + D_3 z e^{-\frac{z^2}{2}}}{2\sqrt{\lambda_0}},$$

where $z = \frac{S}{\sqrt{\lambda_0}}$ is the normalized amplitude of the cycles and the other parameters are as follows:

$$D_1 = \frac{2(x_m - \gamma^2)}{1 + \gamma^2}, \quad D_2 = \frac{1 - \gamma - D_1 + D_1^2}{1 - R}, \quad D_3 = 1 - D_1 - D_2,$$

$$R = \frac{\gamma - x_m - D_1^2}{1 - \gamma - D_1 + D_1^2}, \quad Q = 1.25 \frac{\gamma - D_3 - D_2 R}{D_1},$$

$$x_m = \frac{\lambda_1}{\lambda_0} \sqrt{\frac{\lambda_2}{\lambda_4}}.$$

Despite the lack of a theoretical basis, Dirlik's formula represents the best frequency approximation of the results obtained in the time domain, as confirmed in several papers [15, 16].

MATERIALS AND METHODS

The aim of the experimental tests is to perform random fatigue tests on standard specimens. The specimens that are typically used for constant amplitude axial fatigue tests are described in Standard ASTM-E466-21. In particular, we chose the hourglass specimen geometry, which has a circular cross-section, to be used on both the resonance testing machine and the shaker, and a continuous radius between the ends of the test section, to have a single section with minimum diameter. Figure 1 shows the drawing of the specimen from ASTM Standard and a picture of one of the manufactured specimens, which meets all the requirements on the ratio between test and grip cross-sectional areas, on the test section length, and on the radius of curvature.

The choice of the material was the result of a trade-off between the need to have a fatigue curve low enough to be able to make a relevant fatigue damage even at moderate loads and a yielding stress high enough not to risk reaching it with the overloads that could appear during the random fatigue tests. Figure 2 shows the mechanical properties of the aluminum chosen for the specimen. The tensile test has been carried out on specimens with different shapes and a larger diameter, while the constant amplitude fatigue tests were performed on a resonance testing machine, with fully reversed fatigue loading ($R = -1$) and on specimens of the same type and size as those used for random fatigue tests.

To test specimens with random loads, giving as input the PSD of the load and controlling the test in force, the machine used for testing is the Shaker TIRA vib TV 55240/LS-80 shown in Figure 3. The shaker is commonly used for testing the behavior of mechanical, electrical, and electronic products under the action of dynamic loads whose frequency spectrum is known. It is mounted on a rigid stand

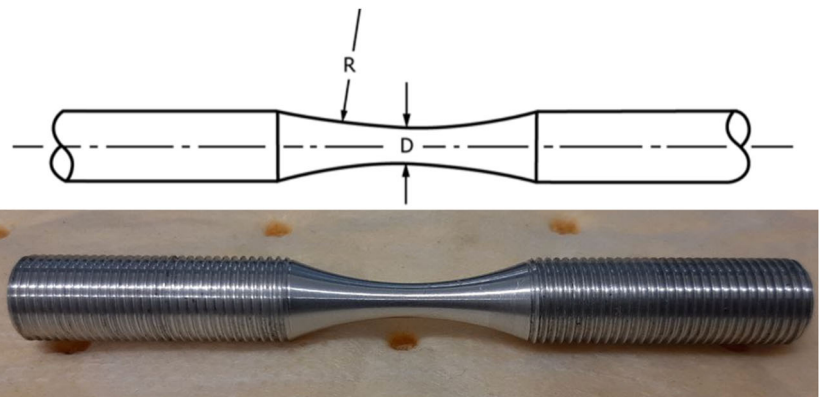


FIGURE 1 Hourglass specimen geometry for axial fatigue tests according to ASTM E466-21 and real specimen ($D = 4$ mm and $R = 36$ mm)

that allows tests in both horizontal and vertical directions. For the purpose of the present study, the shaker is mounted horizontally to allow the bounding of the other end of the specimen to a vertical bench. Figure 3 shows the technical specifications of the shaker, together with its limits. The most important limit to pay attention to during the random fatigue test is the maximum random force, which is equal to 4000 N. This limit is very important to choose the minimum section diameter of the specimen: the chosen diameter was 4 mm so that a maximum peak force of 4000 N, which is equal to the shaker limits, would result in a peak stress of about 318 MPa, low enough not to risk exceeding the yielding stress of the material, but high enough to allow for a certain number of cycles of the random load to be in the HCF part of the fatigue curve.

As previously said, the random fatigue tests are carried out under load control mode. So, a piezoelectric load cell is needed to measure the force during the test and ensure that the shaker applies a force time signal that follows the given PSD. The load cell used for the experimental tests is the ICP Output Force Ring M202B, which has a sensitivity of 0.1256 mV/N and is provided

with a mounting stud that allows to preload the cell to make it work both with tensile and compressive loads. The load cell also supplies a DC reading mode, which allows to measure the preload given to the cell before the test, to guarantee it is in the range requested by the technical specifications of the load cell and that is high enough to avoid separation between the cell and the rest of the test equipment.

One of the drawbacks of using a shaker vibrating machine to perform fatigue tests is that it has no direct methods to detect the fracture of the specimen to immediately stop the test. For this reason, it was decided to perform the random fatigue tests on each specimen in two steps: first, the specimens are mounted on the shaker and are subjected to random loads with a given PSD for an amount of time (calculated by means of preliminary numerical simulations), which should nominally cause a relevant percentage of damage (about 30%); second, the fatigue test is ended on a resonance testing machine to compute the actual residual fatigue life of the specimen. In this way, the result of each test is given in residual percentage damage of the specimen, with respect to the

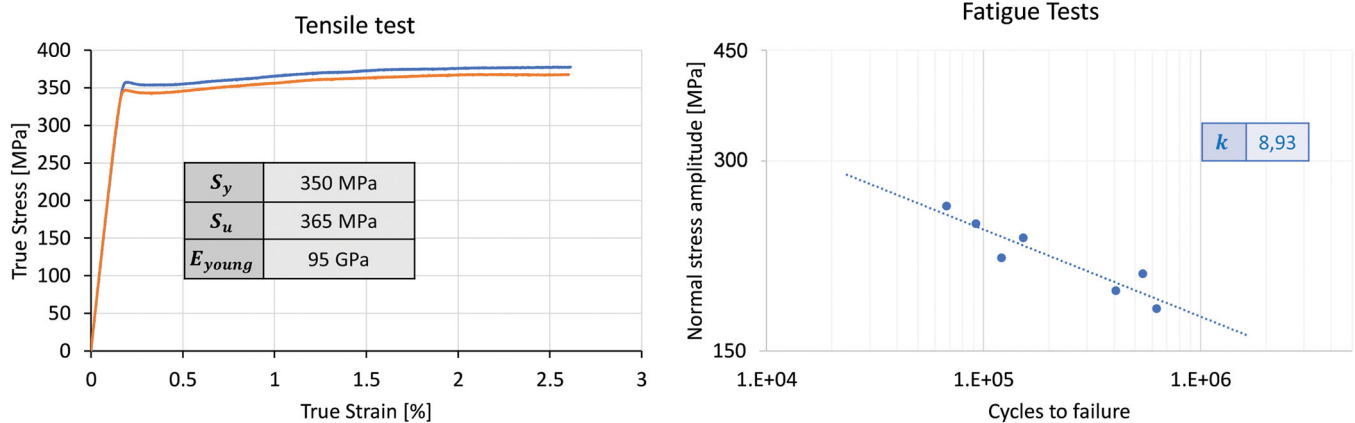


FIGURE 2 Static and fatigue properties of the material used for the specimens



Rated peak force (N lbf)	Sine/Random/Shock	4000/4000/8000	899/899/1798
Frequency range (Hz)		DC-3000	DC-3000
Max. rated travel (mm inch)	Pk-Pk	50.8	2.0
Max. velocity (m/sec inch/sec)	Sine/Random/Shock	1.7/1.7/2.0	67/67/79
Max. acceleration (g)	Sine/Random/Shock	59/59/119	59/59/119
Max. power consumption at 400 V (kVA)		6	6
Nominal impedance (Ohm)		0.9	0.9
Suspension stiffness (N/mm lbf/inch)		50	285.5
Max. weight tested (kg lb)		100	220.5
Effective moving mass (kg lb)		6.8	15.0
Main resonance frequency (Hz)		>3000	>3000
Weight with trunnion (kg lb)		700	1543.2
Stray magnetic field (mT)	without/with degauss kit	<8.5/<0.5	<8.5/<0.5
Armature (ø/mm ø/inch)		180	7.09
Cooling (m ³ /h ft ³ /min)		200	118
Interlocks	Temperature, overtravel, airflow, overcurrent, compressed air		

FIGURE 3 Shaker TIRA vib TV 55240/LS-80 and its technical specifications

fatigue curve of the material, after the random load test. The value of a nominal 30% for the damage was chosen as a trade-off between the need to produce a consistent damage to reduce the influence of fatigue variability on the results, and the need to avoid undesired failures on the shaker and to keep low enough the time required to perform the random test. Obviously, this two-step test presents both other advantages and drawbacks. The main drawback is that making two different tests, also the probability of mounting errors or hitches during the tests doubles, having an impact on the dispersion of test results. On the other hand, the second part of the test with the resonance testing machine allows to accurately and immediately stop the test as specimen failure occurs and it also can be performed with an arbitrary constant amplitude, guaranteeing to break the specimens in the linear part of the bilogarithmic fatigue curve and in a short time. The constant amplitude tests will be performed with the same amplitude of 225 MPa for all the tested specimens which corresponds to a fatigue life of about 10^5 cycles. Moreover, the two machines can be used simultaneously to perform the two parts of the test on two different specimens, so as to further reduce the time needed to carry out the test campaign.

Figure 4a shows the test developed for random fatigue loading, with the shaker locked horizontally and a vertical bench that locks the

specimen on the other end. The connection to the vertical bench is made by clamping a metal plate, on which will be screwed the rest of the equipment (Figure 4b). The position of the plate can be regulated with two regulation screws to ensure coaxiality of the test and avoid bending of the specimen.

Figure 5 shows a section of the full assembly of the equipment and a picture of all the parts included. Components specifically manufactured for this test are colored in orange, while the others are purchased parts (such as the load cell) or pre-existing parts (like the specimen brackets) that are reused to ensure interface also with the resonance testing machine. The equipment consists of: two slotted screws (1) that allow torsional locking of the specimen; two toothed clasps (2) that grip the specimen; two threaded cups (3) that bind the slotted screws to the toothed clasps; a threaded spacer (4) that allows to assemble and disassemble the equipment by screwing into the metal plate on the vertical bench, and a smaller threaded cup (5) that binds the spacer to one of the slotted screws during the test. The connection to the shaker is made with another metal plate constrained with four screws, and on which the mounting stud of the load cell is screwed. In this way, the load cell can be preloaded by tightening one of the slotted screws into the other end of the mounting stud.

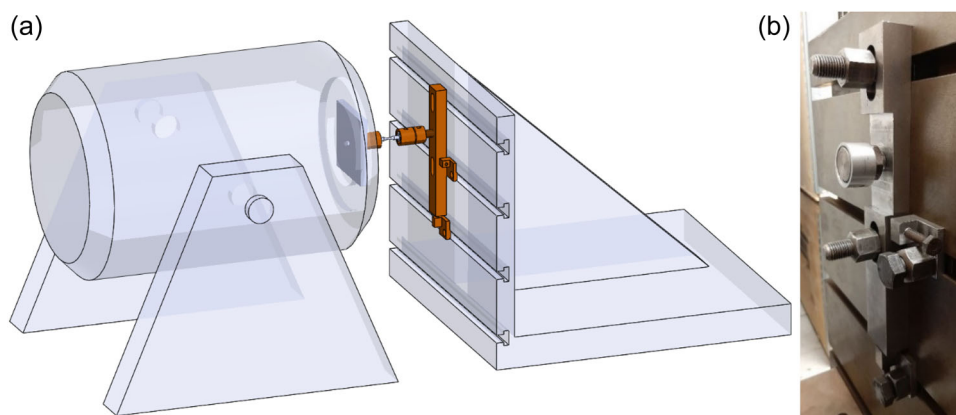


FIGURE 4 Picture of the test bench for the random fatigue test (a) and equipment for specimen interface with the vertical bench (b).

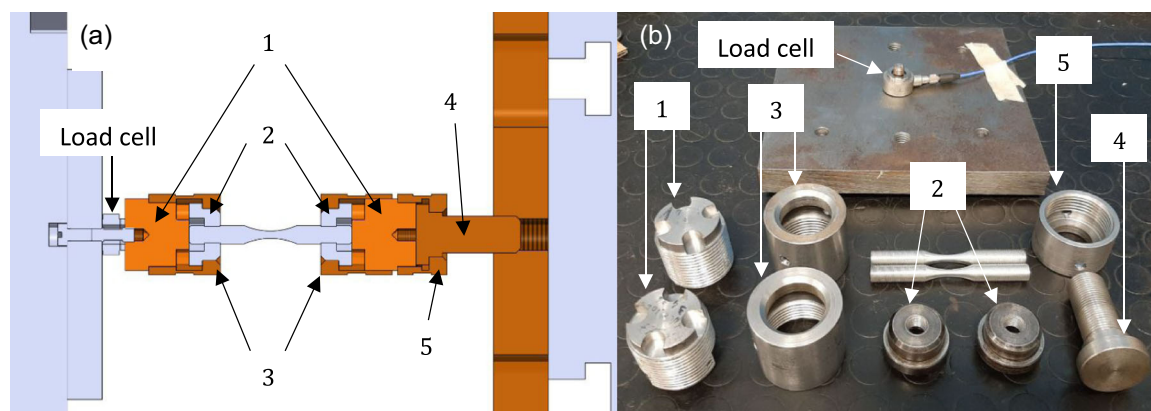


FIGURE 5 Assembly section (a) and picture (b) of the equipment used for the random tests.

EXPERIMENTAL TEST PREPARATION

The mounting procedure of the specimen on the shaker for the random test is shown in Figure 6. To reduce mounting errors, the mounting procedure was kept as similar as possible to that of the resonance machine. In addition, a standardized and repeatable assembly procedure has been established, with as few operations and

disassemblies as possible. The first part of the procedure is carried out down the machine to avoid the torsional preloading of the specimen. One of the slotted screws is clamped to a workbench and one side of the specimen is screwed to the first toothed clasp on it (1); then, the first threaded cup is screwed and tightened with a wrench to secure the first side of the specimen (2). The same procedure is then repeated for the other end of the specimen (3 and 4). Once this first part of the

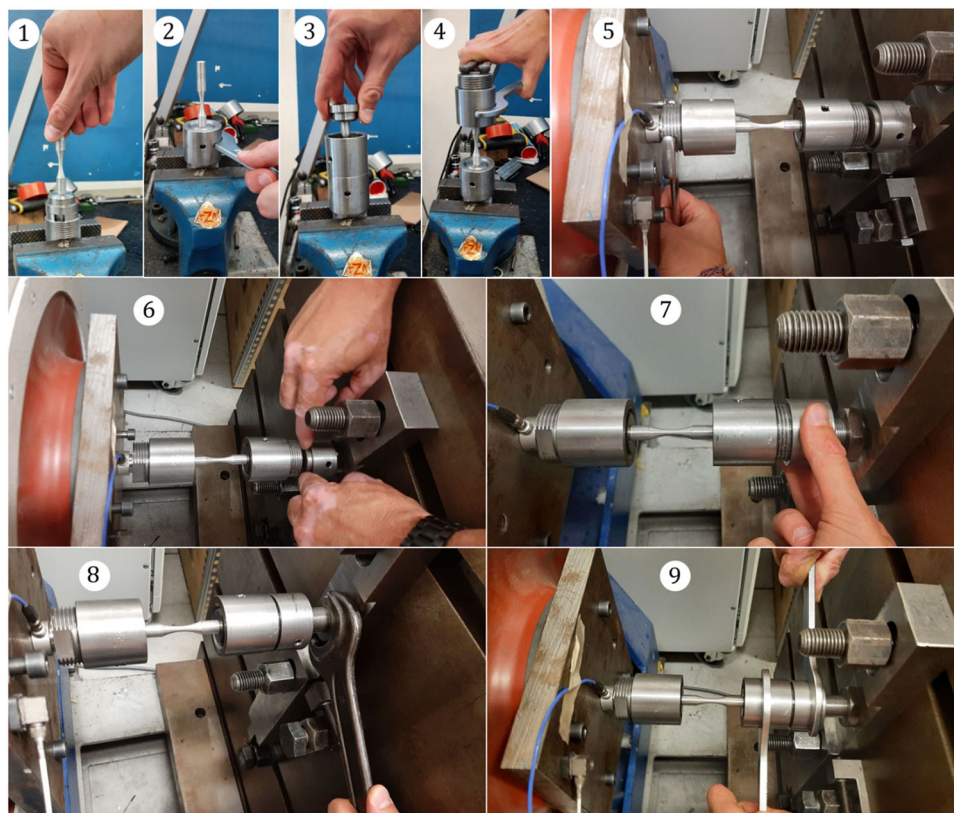


FIGURE 6 Mounting procedure for the random fatigue test

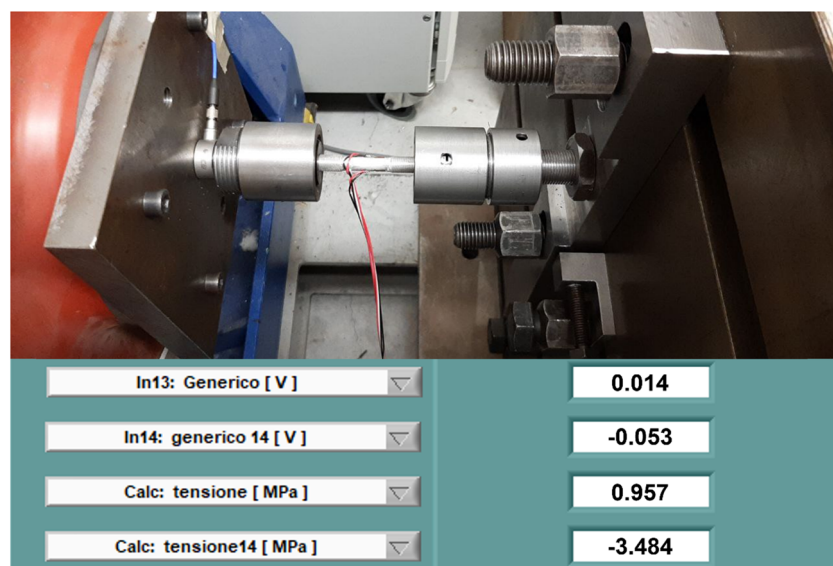


FIGURE 7 Mounting of a specimen with two strain gauges to ensure coaxiality of the test

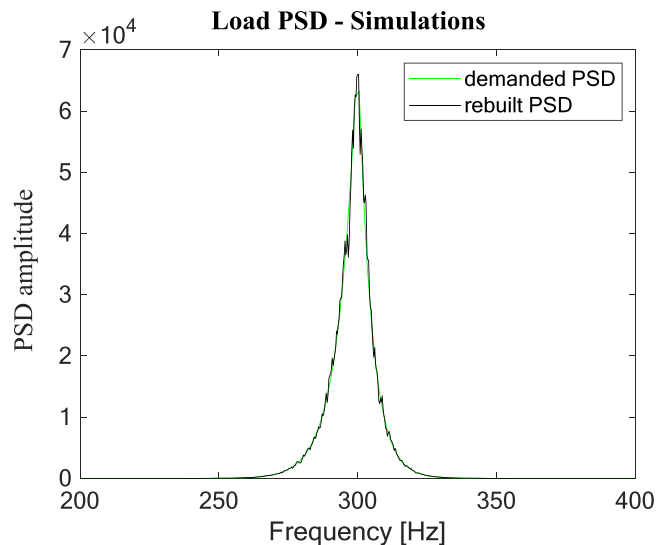


FIGURE 8 Power spectral density of the simulated load

procedure is complete, the equipment can be mounted on the shaker with steps (5)–(9), paying attention to give to the load cell the right preload, which according to the technical specification should be around 8 kN.

As mentioned in the previous section, an important factor of the test assembly and setup is the coaxiality of the parts. In fact, given even the small size of the specimen, a misalignment of the test end constraints would result in the bending of the specimen that would disturb the test results, making it more damaging than expected. To check the alignment of the equipment, a modified specimen was manufactured, two strain gauges were applied on it and it was mounted on the shaker to measure the stress due to bending. After that, the position of the metal plate constrained to the vertical bench has been adjusted using the regulation screws until the stress values measured by the strain gauges were minimized. This procedure is repeated several times rotating the specimen to ensure that the flexural plane does not coincide with the position of the strain gauges. The mounting of the instrumented specimen and the final stress values measured at the end of the centering are shown in Figure 7.

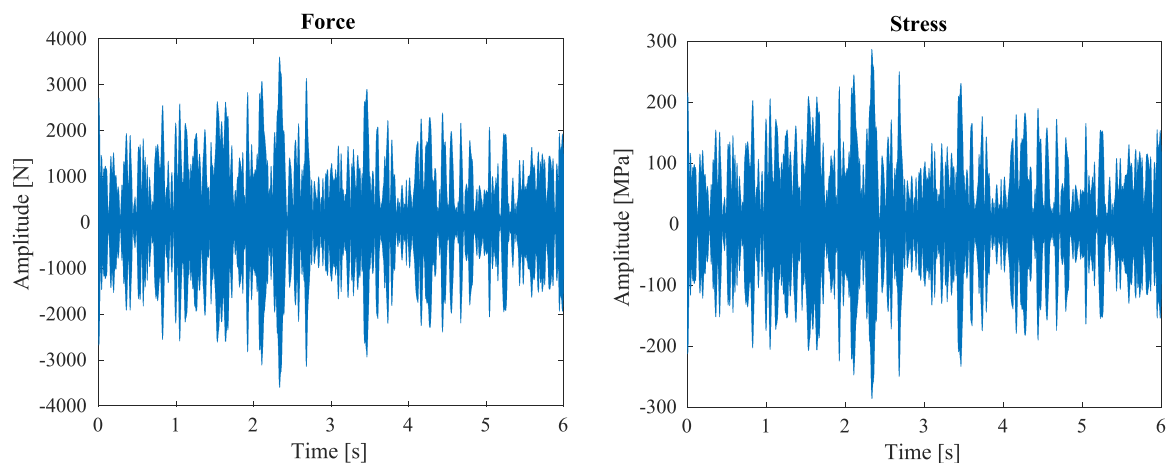


FIGURE 9 Force and stress time histories obtained by numerical simulations

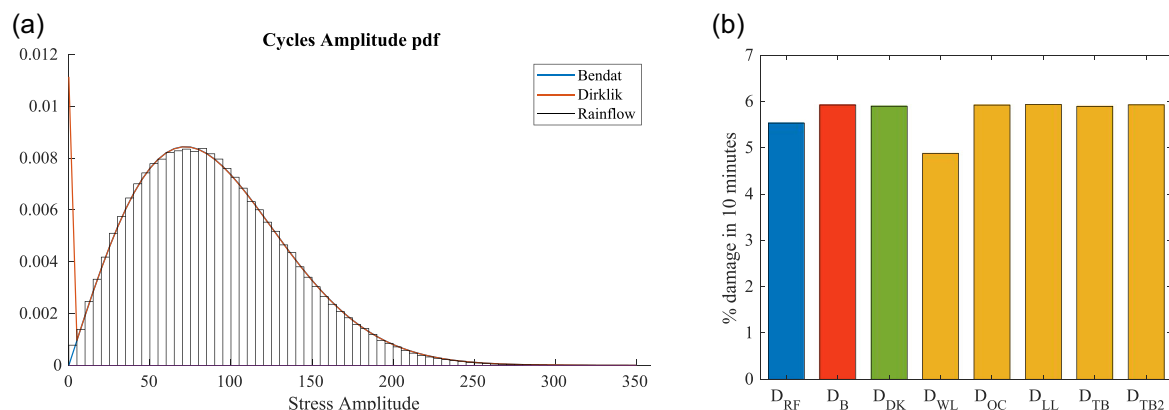


FIGURE 10 Results of numerical simulations in time and frequency domains: probability density function of the amplitudes of the cycles (a) and resulting damage expected after 10 min of load application (b).

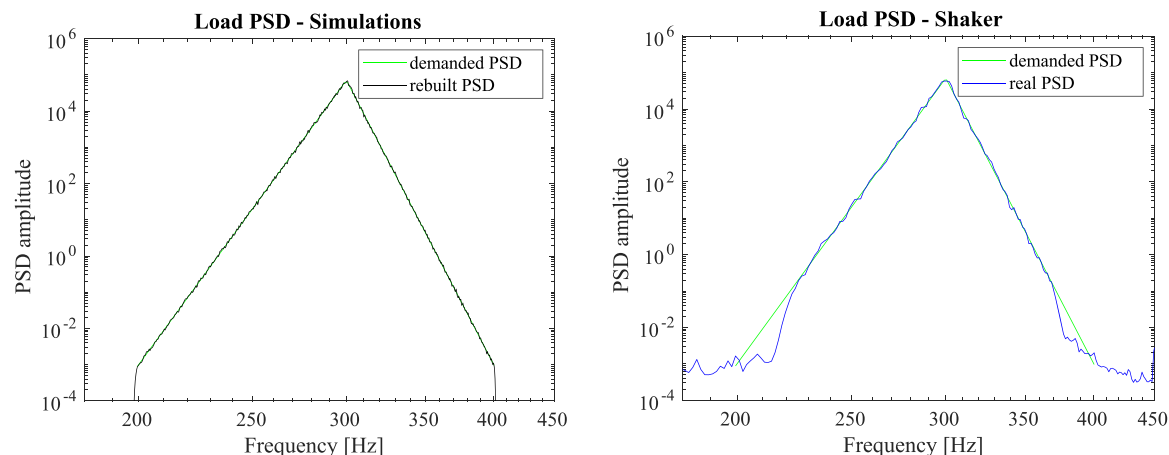


FIGURE 11 Comparison of the power spectral density resulting from numerical simulations and from preliminary experimental test

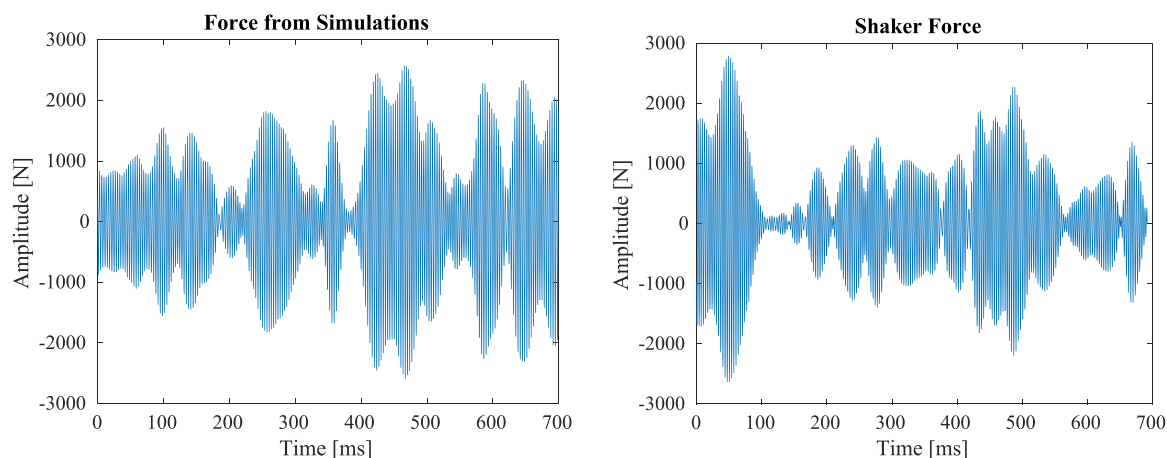


FIGURE 12 Comparison of the load time histories resulting from numerical simulations and from preliminary experimental test

NUMERICAL SIMULATIONS AND PRELIMINARY RESULTS

This section reports the results of some numerical simulations carried out both to calibrate the parameters to be entered into the program for the experimental test and to obtain results to be compared later with the data obtained experimentally. The first step is the choice of the PSD of the load to be applied to the specimens. For these tests, we chose a narrow-band PSD, shown in Figure 8, with a center frequency of 300 Hz, so that a high number of cycles could be applied in a short time, while still not pushing the Shaker to the limit.

The magnitude of the PSD depends on the standard deviation that we want to obtain for our load, which is the square root of the integral of the PSD. The choice of the standard deviation of the load is the result of a trade-off between the need to apply significant damage to the specimen and the need to avoid overloads that could lead both to unexpected failure of the specimen and to exceeding the limits of the shaker. Figure 9 shows the time histories for the force and the stress on the specimen obtained with a standard deviation of

900 MPa: as can be seen, the force does not reach the limit of 4 kN, and the stress keeps well below the yielding stress of the material.

The numerical simulations for fatigue analysis have been performed in both time and frequency domains, and the results are shown in Figure 10. Since the signal is a narrow band (the irregularity factor is 0.99), both Bendat's theory and Dirlik's formula give good approximations of the amplitude pdf of the cycles obtained in the time domain with the rainflow count (Figure 10a). As for the computation of damage, Figure 10b shows that the rainflow method (blue bar) computes a damage of about 5.5% for 10 min of loading. This means that to reach 30% of damage on the specimen, the random test on the shaker should last about 55 min. The red and green bars in Figure 10b are, respectively, the damages computed using the Bendat and Dirlik frequency methods, while the yellow bars are relative to the methods that apply a corrective coefficient to Bendat's damage, described in Wirsching and colleagues [3–6].

Despite lacking full experimental results to be compared to the results from numerical simulations, we managed to perform some preliminary tests on the shaker, whose results are shown in

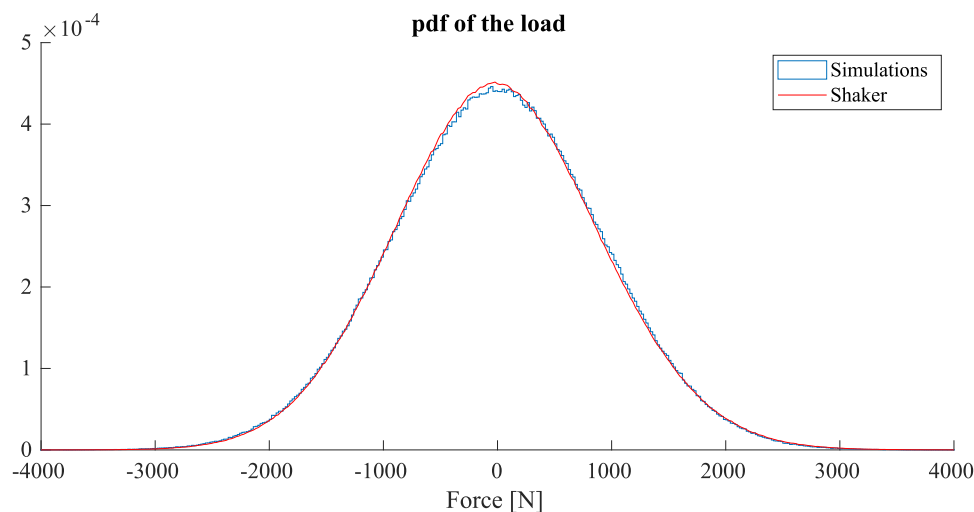


FIGURE 13 Comparison of the load probability density function from numerical simulations and from preliminary experimental test

Figures 11 to 13 along with the corresponding values predicted by the numerical simulations. The PSD of the load applied by the shaker during the experimental test, shown in Figure 11 in the bilogarithmic scale, follows very well the demanded PSD in the central and main part of the frequency span. A small difference can be observed at the ends of the PSD, probably due to the noise of measurements from the load cell. In any case, the PSD values in those areas are very low and the difference can be neglected.

A further demonstration of the good match between the required load and the load actually implemented by the shaker can be seen by comparing the load histories shown in Figure 12. Due to the randomness of the load, the two curves cannot be identical, but it is easily seen how they correspond in terms of loading frequency, modulation of amplitudes, and the amplitude of the applied loads themselves.

Finally, Figure 13 shows the comparison between the load pdfs obtained from simulations and from the preliminary experimental test, which confirms once again that the shaker can accurately reproduce the load required and predicted by the simulations.

CONCLUSIONS

The present paper deals with the definition of a setup to perform experimental random fatigue tests on standard axial fatigue test specimens, to obtain experimental data to compare with the results obtained by frequency methods for fatigue damage computation. The two-step testing procedure involves both a shaker and a resonance testing machine. The setup of the test arrangement is fully described and showed, together with the use of a special specimen equipped with two strain gauges. Reading the tension values on the specimen during assembly allows to adjust the position of the constraint with the vertical bench, thus ensuring coaxiality of the test. However, due to the complex procedure required to ensure proper alignment of

specimens on the shaker, an improvement of the bench is currently under development.

Some numerical simulations are also performed to define the magnitude of the PSD and the duration of the random test to be applied in the future experimental campaign. Finally, the results of numerical simulations are compared to some recordings of a preliminary random test on the shaker, showing a good agreement between the demanded and the real loading conditions.

In conclusion, the present work shows that it is possible to use the shaker similarly to a fatigue machine, even though in an unconventional way, to apply force loads on specimens constrained on both ends. After some minor modifications to afford the alignment problems, the developed apparatus will be used for the experimental characterization of standard hourglass specimens under axial random loadings obtained by various PSD, to achieve experimental data to compare with the results provided by frequency methods.

NOMENCLATURE

γ	irregularity factor
$G(\omega)$	power spectral density
λ_n	spectral moment of n th order
v_0	mean up-crossing rate
v_p	peak rate
ω	angular frequency
$p(S);p(z)$	marginal pdf of cycles' amplitude
σ_x	standard deviation
S	amplitude of the cycles
x_m	normalized central frequency
z	normalized amplitude of the cycles

CONFLICT OF INTEREST

The authors declare no conflict of interest.

DATA AVAILABILITY STATEMENT

Data sharing is not applicable to this article as no data sets were generated or analyzed during the current study.

REFERENCES

- [1] E. H. Vanmarke (1972), *J. Eng. Mech. Div.*, 98(2), 401.
- [2] J. Bendat (1964), Probability functions for random responses, NASA report.
- [3] P. Wirsching, M. Light, *J. Struct. Eng.* **1980**, 106, 1593.
- [4] K. Ortiz, N. Chen. Fatigue damage prediction for stationary wide-band stresses. In *Reliability and Risk Analysis in Civil Engineering, Proc. of the 5th Int. Conf. on the Applications of Statistics and Probability in Soil and Structural Engineering (ICASP5)*, Vancouver, Canada, 25-29 May 1987. Institute for Risk Research, University of Waterloo: Waterloo, ON, Canada, **1987**.
- [5] C. E. Larsen, L. D. Lutes, *Probabilistic Eng. Mech.* **1991**, 6, 96.
- [6] D. Benasciutti, R. Tovo, *Int. J. Fatigue* **2005**, 27, 867.
- [7] T. Dirlik, PhD Thesis, University of Warwick (Coventry) **1985**.
- [8] I. Richlik, *Int. J. Fatigue* **1987**, 9(2), 119.
- [9] A. Niesłony, M. Růžicka, J. Papuga, A. Hodr, M. Balda, J. Svoboda, *Int. J. Fatigue* **2012**, 44, 74.
- [10] D. Marques et al., *Fatigue Fract. Eng. Mater. Struct.* **2021**, 1, 13439.
- [11] D. Gao, W. Yao, W. Wen, J. Huang, *Int. J. Fatigue* **2021**, 148, 106235.
- [12] Y. Wang, R. Serra, *Sensors* **2021**, 21(21), 4518.
- [13] M. Palmieri, G. Zucca, G. Morettini, L. Landi, F. Cianetti, *Materials* **2022**, 15(15), 854.
- [14] S. O. Rice, *Bell Syst. Tech. J.* **1944**, 23, 282.
- [15] C. Braccesi, F. Cianetti, G. Lori, D. Pioli, *Int. J. Fatigue* **2005**, 27, 335.
- [16] D. Benasciutti, R. Tovo, *Probabilistic Eng. Mech.* **2006**, 21, 287.
- [17] W. Zhao, M. Baker, *Int. J. Fatigue* **1992**, 14(2), 121.
- [18] S. Sakai, H. Okamura, *Int. J. Ser. A* **1995**, 38(2), 440.

How to cite this article: M. Sgamma, A. Chiocca, F. Bucchi, F. Frendo, *Appl. Res.* **2023**, e202200066.
<https://doi.org/10.1002/appl.202200066>